Accepted Manuscript

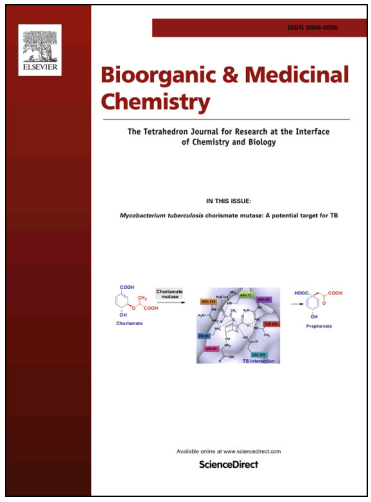

C-2 (E)-4-(Styryl)aniline Substituted Diphenylpyrimidine Derivatives (Sty-DPPYs) as Specific Kinase Inhibitors Targeting Clinical Resistance related EGFR^{T790M} Mutant

Anran Song, Jianbin Zhang, Yang Ge, Changyuan Wang, Qiang Meng, Zeyao Tang, Jinyong Peng, Kexin Liu, Yanxia Li, Xiaodong Ma

PII: S0968-0896(17)30335-8
DOI: http://dx.doi.org/10.1016/j.bmc.2017.03.032
Reference: BMC 13630

To appear in: *Bioorganic & Medicinal Chemistry*

Received Date: 18 February 2017
Revised Date: 14 March 2017
Accepted Date: 16 March 2017

Please cite this article as: Song, A., Zhang, J., Ge, Y., Wang, C., Meng, Q., Tang, Z., Peng, J., Liu, K., Li, Y., Ma, X., *C*-2 (E)-4-(Styryl)aniline Substituted Diphenylpyrimidine Derivatives (Sty-DPPYs) as Specific Kinase Inhibitors Targeting Clinical Resistance related EGFR^{T790M} Mutant, *Bioorganic & Medicinal Chemistry* (2017), doi: http://dx.doi.org/10.1016/j.bmc.2017.03.032

Bioorganic & Medicinal Chemistry
journal homepage: www.elsevier.com

C-2 (E)-4-(Styryl)aniline Substituted Diphenylpyrimidine Derivatives (Sty-DPPYs) as Specific Kinase Inhibitors Targeting Clinical Resistance related EGFR^{T790M} Mutant

Anran Song[a,1], Jianbin Zhang[a,1], Yang Ge[a], Changyuan Wang[a], Qiang Meng[a], Zeyao Tang[a], Jinyong Peng[a], Kexin Liu[a], Yanxia Li[b] and Xiaodong Ma[a,*]

[a] *College of Pharmacy, Dalian Medical University, Dalian 116044, PR China.*
[b] *Department of Respiratory Medicine, the First Affiliated Hospital of Dalian Medical University, Dalian 116011, PR China.*
[1] *These authors contributed equally to this work.*
[*] *Corresponding author.*
Email address: xiaodong.ma@139.com (X. Ma).

ARTICLE INFO

Article history:
Received
Received in revised form
Accepted
Available online

Keywords:
NSCLC
Resistance
EGFR^{T790M}
Inhibitor
Diphenylpyrimidine

ABSTRACT

With the aim to overcome the drug resistance induced by the EGFR T790M mutation (EGFR^{T790M}), herein, a family of diphenylpyrimidine derivatives (Sty-DPPYs) bearing a *C*-2 (*E*)-4-(styryl)aniline functionality were designed and synthesized as potential EGFR^{T790M} inhibitors. Among them, the compound **10e** displayed strong potency against the EGFR^{T790M} enzyme, with the IC_{50} of 11.0 nM. Compound **10e** also showed a higher SI value (SI = 49.0) than rociletinib (SI = 21.4), indicating its less side effect. In addition, compound **10e** could effectively inhibit the proliferation of H1975 cells harboring the EGFR^{T790M} mutation, within the concentration of 2.91 μM. Significantly, compound **10e** has low toxicity against the normal HBE cell (IC_{50} = 22.48 μM). This work provided new insights into the discovery of potent and selective inhibitor against EGFR^{T790M} over wild-type (EGFR^{WT}).

1. Introduction

Non-small cell lung cancer (NSCLC) accounts for approximately 85% of all lung cancers, with the 5-year survival rate of less than 5%.[1-3] The standard treatment for advanced NSCLC is a combination of platinum compounds and taxanes, however, the treatment is associated with severe adverse effects, low selectivity and high toxicity.[4-6] In recent decades, the application of target-specific agents to treat patients with lung cancer has shown impressive therapeutic effects in clinical trials, especially the agents targeting to the activating mutations of epidermal growth factor receptor (EGFR). EGFR, existing on the cell surface, is a member of the ErbB family of receptors. It plays an important role in many signaling processes, that regulate numerous cellular functions of cell growth, differentiation, and angiogenesis.[7,8] The mutations of EGFR, which lead to its overexpression or overactivity, are associated with various cancers.[9]

EGFR mutations account for approximately 10-15% of NSCLC cases in North America and Europe, and 30-40% of NSCLCs in Asian countries.[10] Gefitinib (**1**, Fig.1)[11,12] and erlotinib (**2**, Fig.1)[13], the first generation of EGFR tyrosine kinase inhibitors (TKIs), have shown good response rates in NSCLC patients with activating $EGFR^{Del\ 19}$ or $EGFR^{L858R}$ mutations. Compared with platinum-based chemotherapy, they conferred excellent radiographic overall response rates of 50-75%, improved progression-free survival by 8-14 months and improved the quality of life.[14] Unfortunately, the clinical efficacy of gefitinib and erlotinib is diminished because patients have developed resistance within 10-16 months.[15] In particular, approximately 60% of the patients who have developed resistance are associated with a single second-site EGFR kinase domain mutation at the gatekeeper position (Thr^{790} to Met^{790}, T790M).[16,17] The second-generation EGFR-TKIs (such as afatinib, **3**, Fig.1) are developed to overcome the acquired resistance after the failure of the first generation of EGFR-TKIs. Despite the promising cellular potency against the $EGFR^{T790M}$ mutation, afatinib exhibits insufficient efficacy in patients at clinically achievable concentrations. The non-selectivity against wild-type EGFR ($EGFR^{WT}$) and mutant EGFR could lead serious epithelium-based toxicities such as rash and diarrhea, which have limited the clinical application of afatinib.[18] Hence, there is an urgent need for EGFR-TKIs that can selectively identify and inhibit the $EGFR^{T790M}$ mutation, while also leaving the wild-type form of EGFR.

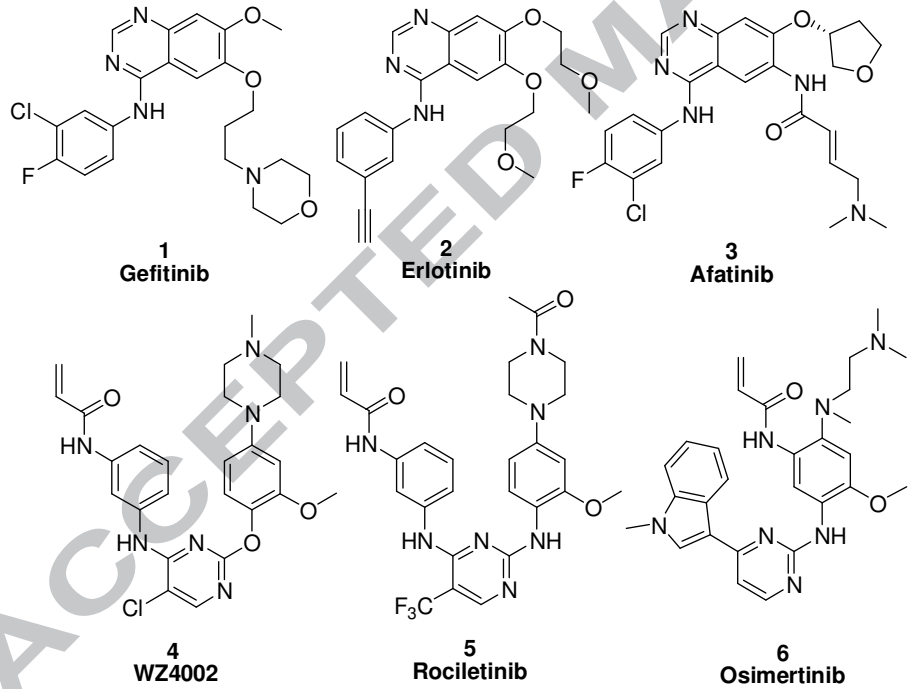

Figure 1. Chemical structures of the novel EGFR inhibitors

Recently, the third-generation EGFR-TKIs including WZ-4002 (**4**)[19], rociletinib (CO-1686, **5**)[20] and osimertinib (AZD9291, **6**)[21,22], have been developed with high potency against T790M-containing mutants and selectivity over the wild-type EGFR (Fig.1). They have demonstrated a high and sustained response in patients with advanced EGFR-mutant NSCLC who have experienced treatment failure with first- and second-generation EGFR-TKIs. Osimertinib was approved by the United States Food and Drug

Administration agency in late 2015, and rociletinib is undergoing phase III clinical trial evaluation. Generally, a common pyrimidine structure core, which could interact with the hinge residue Met793 by forming a bidentate hydrogen bonding interaction, is essential for the third-generation EGFR inhibitors to maintain the high anti-EGFR^{T790M} activity. Moreover, a Michael addition receptor moiety, acrylamide, is also necessary to form a covalent binding with the conserved cysteine residue present in the lip of the EGFR ATP binding site (Cys797).[19]

The stilbene group is a novel biological functionality, contained in several molecules, such as resveratrol (**7**)[23], diethylstilbestrol (**8**)[24], and pterostilbene (**9**)[25] (Fig.2). The typical agent, resveratrol, has been widely reported to possess bioactivities of anti-inflammatory, anticancer, antiviral, antioxidant and neuroprotective bioactive effects. As anticancer agents, resveratrol and its analogues inhibit the activity of tyrosinase and induce the apoptosis and autophagy of NSCLC cells.[23] Remarkably, resveratrol has been reported to overcome the acquired resistance of NSCLC cells when treated in combination with gefitinib. Accordingly, we hypothesized that EGFR-TKIs combined with the *trans*-stilbene structure might have a synergistic effect on inhibiting the EGFR mutation. In this study, a series of pyrimidine derivatives bearing a *trans*-stilbene group were designed and synthesized to discover more effective EGFR^{T790M} inhibitors (Fig.2). In addition, their anti-EGFR^{T790M} activities were also evaluated by *in vitro* kinase enzymatic assay and cellular activity assay.

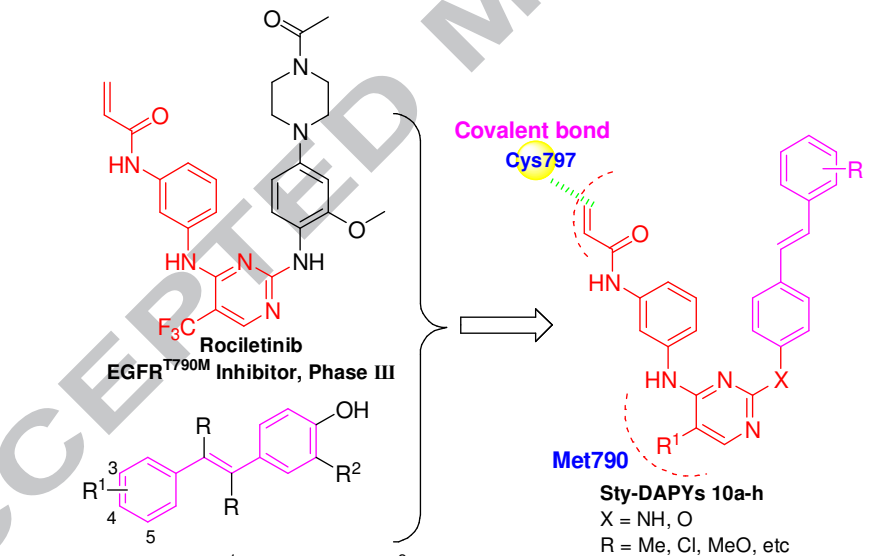

Figure 2. Designed strategy of the Sty-DPPY derivatives.

2. Results and discussion

2.1. Chemistry

The designed compounds **10a-h** were prepared following the general strategy outlined in Scheme 1.[26,27] Briefly, a family of benzyl bromide derivatives **11a-d** were reacted with the nucleophilic reagent triethyl phosphate to generate intermediates **12a-d**, which were then reacted with *p*-nitrobenzaldehyde following

the Wittig-Horner reaction to produce the (*E*)-4-nitrostilbene analogues **13a-d**. Subsequently, the nitro substituent in compounds **13a-d** was reduced by Fe-NH_4Cl to form the (*E*)-4-aminostilbene intermediates **14a-d**. Additionally, 3-aminophenol and *m*-phenylenediamine materials **15a-b** were reacted with acryloyl chloride to prepare the 3-(*N*-acrylamide)amines **16a-b**. After regioselectively coupling with the 4-chloro group of the 2,4-dichloropyrimidine core, the amino-substituted compounds **16a-b** were conveniently converted to the pyrimidines **17a-d**. Finally, the desired aminopyrimidines derivatives containing the (*E*)-4-nitrostilbene group **10a-h** were synthesized when coupled by flexible construction containing the (*E*)-4-aminostilbene group with the pyrimidine framework **17a-d**.

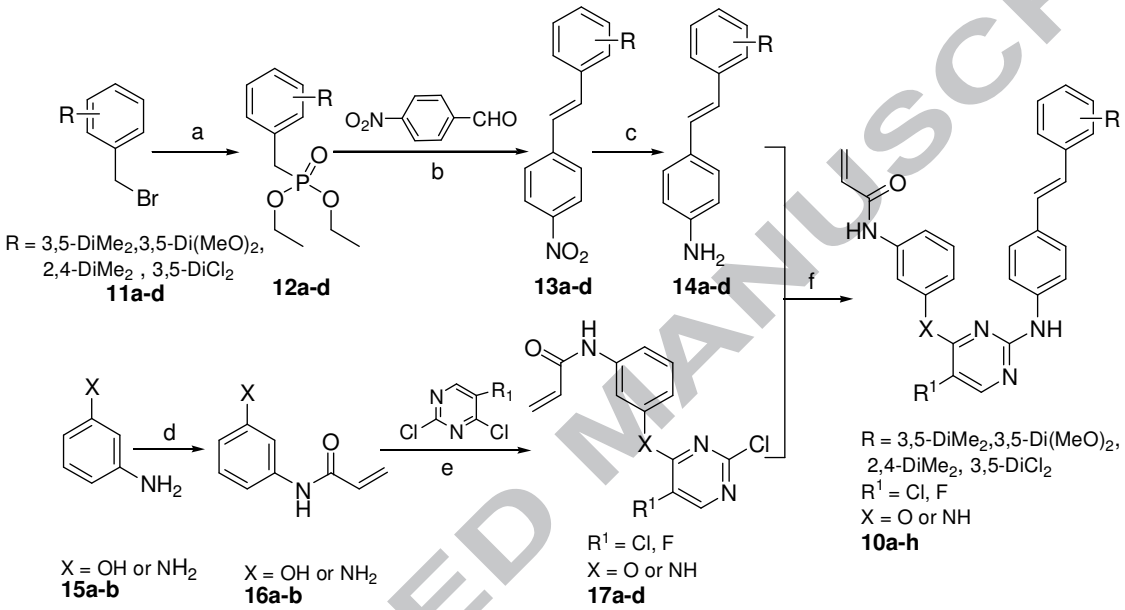

Scheme 1. Synthetic route of the title compounds **10a-h**. Reagents and conditions: (a) $P(OEt)_3$, *n*-Bu_4NBr, 150 °C, reflux, 6 h, 82-91%; (b) *p*-nitrobenzaldehyde, CH_3ONa, DMF, 0 °C to rt., overnight, 68-88%; (c) Fe-NH_4Cl, MeOH-H_2O, 2 h, 70 °C, 78-92%; (d) acryloyl chloride, $NaHCO_3$, CH_3CN, rt., 0.5 h, 93-95%; (e) DIPEA, 1,4-dioxane, rt., 2 h, 88-91%; (f) trifluoroacetic acid, 2-BuOH, 100 °C, 12 h, 30.5–68.5%.

2.2. Biological activity

2.2.1. Kinase inhibitory activity

All the Sty-DPPY derivatives were evaluated for their activities against the wild-type EGFR and the T790M/L858R-mutated EGFR applying with the ADP-Glo™ kinase assay system.[28,29] Two novel agents, gefitinib and rociletinib, were also tested as positive controls. The results of this evaluation, shown in Table 1, obviously revealed that Syt-DPPYs have strong inhibitory activity against the mutant $EGFR^{T790M/L858R}$, with IC_{50} values in the range of 6.8 to 26.5 nM. In contrast, this class of inhibitors displayed the potency to inhibit $EGFR^{T790M/L858R}$ activity 21 to 57 times higher than gefitinib. Among them, four typical compounds **10e** (IC_{50} = 11.0 nM), **10f** (IC_{50} = 6.8 nM), **10g** (IC_{50} = 8.1 nM), **10h** (IC_{50} = 11.3 nM), still exhibited stronger activity than rociletinib (IC_{50} = 21.5 nM). Structure and activity relationship (SAR) analysis showed that substituents installed on the *C*-2 (E)-4-(styryl)aniline slightly affect their anti-

$EGFR^{T790M/L858R}$ activity. Generally, the 2,4-disubtituted compound **10f** was superior than **10d** (26.5 nM) with 3,5-disubstituents. In addition, Sty-DPPYs exhibited moderate activity against the wild-type EGFR with the IC_{50} values ranging from 51.3 to 1037 nM. It was evident that compounds **10f** and **10h** had the least potency against the wild-type EGFR, with IC_{50} values of 996.1 nM and 1037 nM, respectively. In particular, inhibitor **10f**, which had a SI value of 146.5, displayed higher selectivity than rociletinib. Moreover, compounds **10e** (SI = 49.0), **10g** (SI = 47.7), and **10h** (SI = 91.8) also had improved selectivity, indicating their less side effects.

Table 1
In vitro enzymatic inhibitory activity of compounds **10a-h** against $EGFR^{WT}$ and $EGFR^{790M/L858R}$.

Compd.	R	R^1	X	EGFR IC_{50} (nM) [a]		
				WT	T790M/L858R	SI (WT:T790M/L858R)
10a	3,5-$DiMe_2$	Cl	O	87.0	22.4	3. 9
10b	3,5-$DiCl_2$	F	N	388.1	14.2	27.3
10c	3,5-diMeO_2	Cl	N	216.1	15.7	13.8
10d	3,5-$DiMe_2$	Cl	N	606.5	26.5	22. 9
10e	3,5-$DiMe_2$	F	N	539.2	11.0	49.0
10f	2,4-$DiMe_2$	Cl	N	996.1	6.8	146.5
10g	2,4-$DiMe_2$	F	N	386.7	8.1	47.7
10h	3,5-$DiCl_2$	Cl	N	1037	11.3	91.8
gefitinib	_	_		10.6	1202	0.009
rociletinib	_	_		460.2	21.5	21.4

[a] EGFR activity assays were performed using the ADP-Glo™ Kinase Assay according to the manufacturer's instructions. The compounds were incubated with the kinase reaction mixture for 1h before measurement. The data were means from at least three independent experiments.

2.2.2. Cellular antiproliferative activities

Table 2
Antiproliferative activity of compounds **10a-h** against cells harboring a different status of EGFR.

Compd.	Cellular antiproliferative activity (IC_{50}, μM) [a]				
	A431	H1975	A549	HCC827	HBE
10a	4.71	13.73	10.75	11.66	6.07
10b	1.29	6.98	7.01	10.79	5.42
10c	1.78	3.76	6.84	3.32	9.18
10d	5.56	2.32	5.59	4.00	17.01
10e	10.55	2.91	12.81	2.07	22.48
10f	3.16	4.39	4.94	9.71	15.83
10g	3.11	7.16	1.32	>20	10.44

10h	6.56	6.98	15.83	9.16	35.2
gefitinib	6.12	13.13	36.21	0.0099	17.64
rociletinib	1.79	0.137	3.24	0.031	23.80

[a] The inhibitory effects of individual compounds on the proliferation of cancer cell lines were determined by the MTT assay. The data were means from at least three independent experiments.

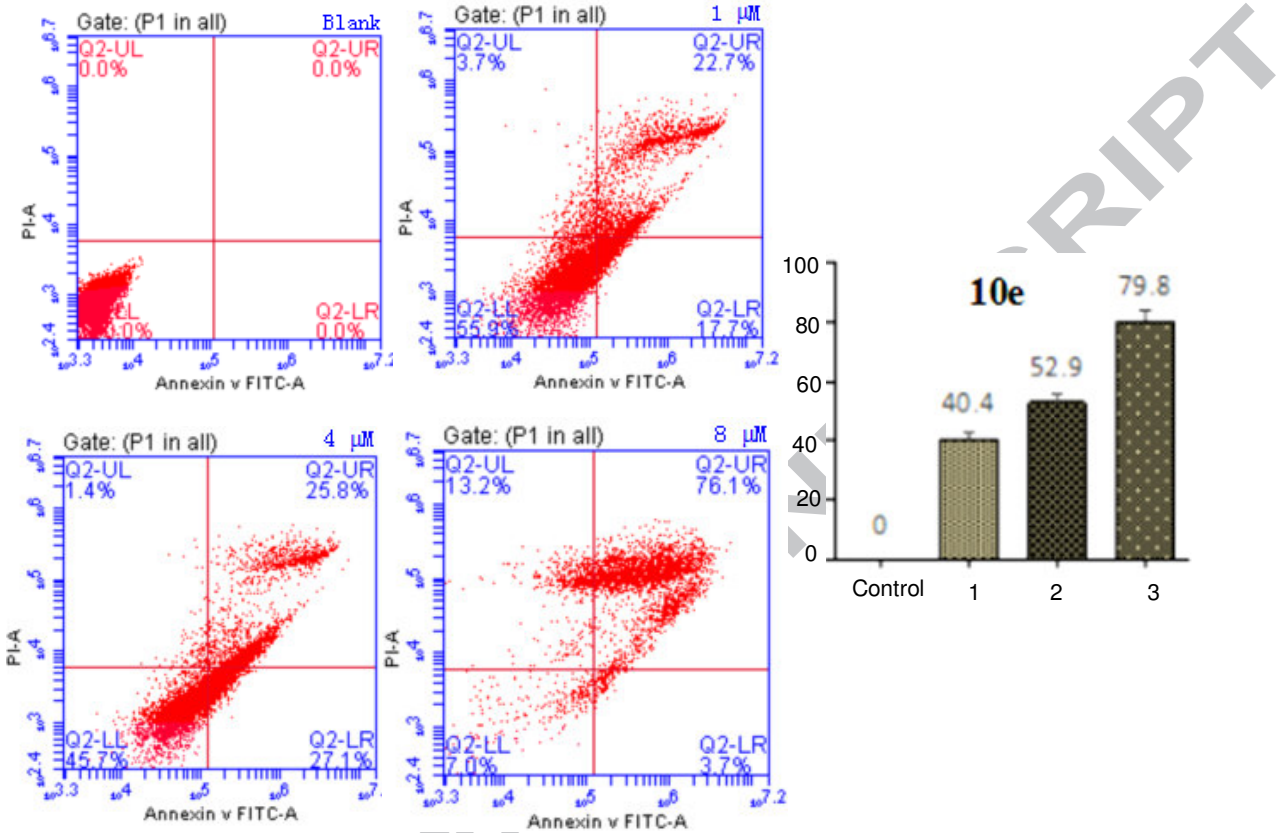

Figure 3. Compound **10e** induced H1975 cell apoptosis *in vitro*. The cells were incubated with the indicated concentrations of **10e** for 72 h, and the cells were stained with annexin V/FTIC, followed by flow cytometry analysis. One representative experiment is shown.

The antiproliferative activities of these newly synthesized compounds were also investigated by the MTT assay in four NSCLC cell lines (A431, H1975, A549 and HCC827), and one normal lung cell line (HBE). A431 cells have the wild-type EGFR, while H1975, A549 and HCC827 cells harbor different EGFR mutations (H1975 harboring $EGFR^{L858R/T790M}$ mutation, A549 harboring $EGFR^{K\text{-}ras}$ mutation, and HCC827 harboring $EGFR^{del\ E746\text{-}A750}$ mutation). The two novel agents, gefitinib and rociletinib, were studied as references. As seen in Table 2, Sty-DPPYs are able to inhibit H975 cells within micromolar concentrations, with IC_{50} values in the range of 2.32 μM to 13.73 μM. Among them, compounds **10d** and **10e** were the most potent inhibitors against H1975 cells, with IC_{50} values of 2.32 μM, 2.91 μM, respectively. While for the activity against the wild-type A431 cells, compounds **10d** and **10e** have IC_{50} values of 5.56 μM and 10.55 μM, revealing that both **10d** and **10e** have weak selectivity against resistant H1975 cells over wild-type A431 cells. Notably, inhibitor **10e** also displayed the strongest potency for inhibiting the replication of HCC827 cells among this class of inhibitors, with an IC_{50} value of 2.07 μM. Interestingly, the 2,4-dimethyl-substituted analogue **10g** could interfere with the K-ras mutated A549 cells at a low concentration

of 1.32 μM. The activity against the normal HBE cells showed that most of Sty-DPPYs have weak inhibitory capability, indicating that they will produce low cytotoxicity. In particular, the most active inhibitor **10e** still has the lowest activity for inhibiting HBE cells (IC_{50} = 22.48 μM), exhibiting excellent biological property for the further development. Additionally, the effects of inhibitor **10e** on apoptosis in the H1975 cell line were also explored using flow cytometry analysis. The inhibitory effects of molecule **10e** were clearly increased in a concentration dependent manner, with an apoptosis rate ranging from 40.4 to 79.8%, as shown in Figure 3.

2.3. Molecular modelling analysis

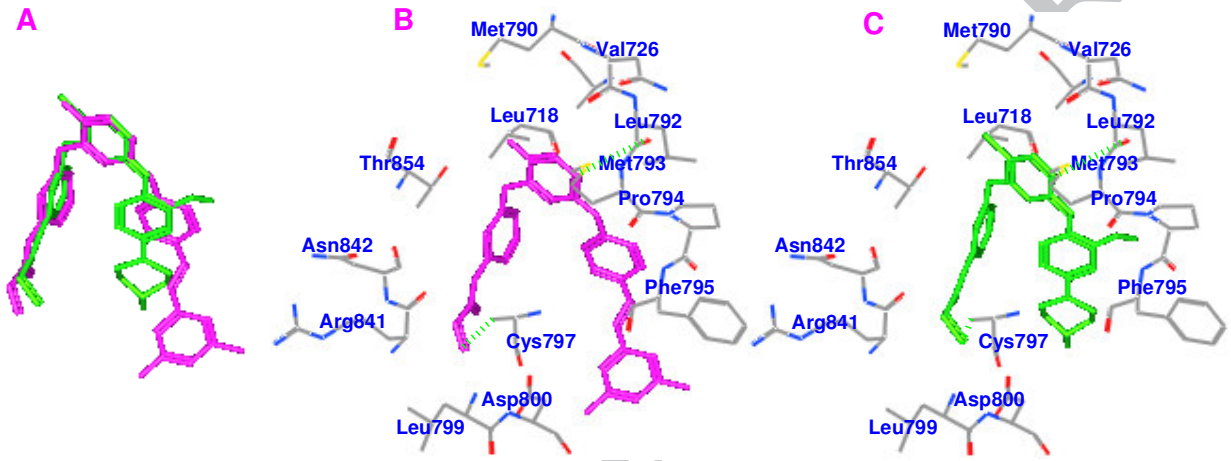

Figure 4. A) Conformation alignment of WZ4002 and inhibitor **10e;** B) binding mode of WZ4002 within $EGFR^{T790M}$ enzyme (PDB code: 3IKA); C) putative binding mode of **10e** within $EGFR^{T790M}$.

Additionally, the most active inhibitor **10e** was docked into the ATP binding pocket of $EGFR^{T790M}$ (PDB: 3IKA)[19] to investigate the putative interaction mechanism with the EGFR target. The software AutoDock 4.2 was used with its default parameters.[30-31] For comparison, the x-ray crystal conformation of the lead compound WZ4002 was reserved and analyzed as well. As shown in Figure 4, both the typical Sty-DPPY **10e** and WZ4002 could tightly contact with EGFR kinase in an identical manner, including: (1) covalent bond forces produce by the acryl amide group with the amino acid Cys797; (2) strong contacts come from the chlorine atom at the *C*-5 position of the pyrimidine core with the mutant gatekeeper residue Met790; (3) hydrogen-bond forces generated from the *N*-1 nitrogen atom of the pyrimidine core with amino acid Met793; (4) polar forces formed by the piperazine ring with the outside of the ATP-binding pocket of $EGFR^{T790M}$. For inhibitor **10e**, the phenyl ring in the *C*-2 (*E*)-4-(styryl)aniline moiety formed additional strong π-π contacts with the amino acid Phe795, which might improve the inhiibitory activity against the$EGFR^{T790M}$ activity. Overall, this docking model was consistent with the biological activity data.

3. Conclusion

Based on the pyrimidine template, a series of *C*-2 (*E*)-4-(styryl)aniline substituted Sty-DPPYs were synthesized and evaluated as potent $EGFR^{T790M}$ mutant inhibitors. In particular, compound **10e** displayed

strong anti-EGFR^{T790M} activity (IC_{50} =11.0 nM), while its effect on the wild-type EGFR (IC_{50} = 49.0 nM) was significantly less potent. Apparently, compound **10e** showed higher selectivity and stronger potency than the novel agent rociletinib. Moreover, inhibitor 10e could interfere with the proliferation of H1975 cells at a concentration of 2.91 μM, and had little effect on the normal HBE cells at this concentration. Flow cytometry analysis demonstrated that **10e** could significantly induce the apoptosis (52.9%) of H1975 cell at a concentration of 4 μM. Overall, the results obtained with compound **10e** suggested that it might be used as a lead compound for further development as a selective EGFR inhibitor to overcome resistance effects conferred by the EGFR mutations.

4. Experimental section

4.1. General Methods and Chemistry.

All commercial chemicals and solvents were analytical grade and were used without further purification. High resolution ESI-MS were performed on an AB Sciex TripleTOF® 4600 LC/MS/MS system. ^{1}H NMR and ^{13}C NMR spectra on a Brucker AV 400 MHz spectrometer were recorded in [*d*]DMSO. Coupling constants (*J*) are expressed in hertz (Hz). Chemical shifts (δ) of NMR are reported in parts per million (ppm) units relative to internal control (TMS). All reactions were monitored by TLC, using silica gel plates with fluorescence F254 and UV light visualization. Flash chromatography separations were obtained on Silica Gel (300–400 mesh) using dichloromethane/methanol as eluents.

4.2. General procedure for the synthesis of 10a–j.[26,27]

Compounds **14a-d** were synthesized according to our previously reported procedure. While compounds **17a-d** were prepared using the reported mehthod[32,33]. All these intermediates were used without any purification. With these intermediates in hand, the newly obtained compounds were synthesized as described below. A flask was charged with compounds **14a-d** (0.70 mmol), **17a-d** (0.70 mmol), TFA (0.08 mL, 1.05 mmol), and 2-BuOH (10 mL).The slurry was heated to 100 °C for 5 h. The reaction mixture was allowed to cool to room temperature and was neutralized with a saturated aqueous sodium bicarbonate solution. The aqueous mixture was then extracted with CH_2Cl_2 (20 mL) three times. The crude product was purified using flash chromatography with dichloromethane/methanol (v/v, 30:1) as eluents.

_N_-[3-[[5-Chloro-2-[(*E*)-4-(3,5-dimethylstyryl)phenylamino]-4-pyrimidinyl]amino]phenyl]-2-acrylamide (10a)

Yield 30.5%; deep yellow solid; ^{1}H NMR (DMSO-d_6): δ 2.28(s, 6H), 5.76-5.79 (d, *J* = 12 Hz, 1H), 6.26-6.30 (d, *J* = 16 Hz, 1H), 6.43-6.50 (m, 1H), 6.87-7.08 (m, 4H), 7.16 (s, 2H), 7.25-7.51 (m, 5H), 7.65-7.69 (m, 2H), 8.50 (s, 1H), 9.90 (s, 1H), 10.46 (s, 1H); ^{13}C NMR (DMSO-d_6): δ 21.43 (2C), 105.27, 113.49, 117.29, 117.53, 119.27, 124.53 (2C), 126.85, 126.91 (2C), 127.88, 128.17, 129.34, 130.54, 131.11, 132.15,

137.63, 138.05 (2C), 139.68, 140.90, 152.79, 157.84, 158.63, 163.90 (2C), 164.38; HRMS (ESI^+) for $C_{29}H_{25}ClN_4O_2$, $[M+H]^+$ calcd: 497.1739, found: 497.1749.

***N*-[3-[[5-Fluoro-2-[(*E*)-4-(3,5-dichlorostyryl)phenylamino]-4-pyrimidinyl]amino]phenyl]-2-acrylamide (10b)**

Yield 44.6%; light gray solid; ^1H NMR (DMSO-d_6): δ 5.73-5.76 (d, J =12 Hz, 1H), 6.24-6.29 (d, J = 20 Hz, 1H), 6.46-6.53 (m, 1H), 7.03-7.07 (d, J = 16 Hz, 1H), 7.33-7.37 (m, 2H), 7.44-7.52 (m, 5H), 7.60-7.63 (d, J = 12 Hz, 4H), 7.99 (s, 1H), 8.23-8.24 (d, J = 4 Hz, 1H), 9.90 (s, 1H), 10.19 (s, 1H), 10.29 (s, 1H); ^{13}C NMR (DMSO-d_6): δ 114.84, 116.56, 118.88, 120.39 (2C), 124.16, 125.10 (2C), 126.69, 127.51, 127.77 (2C), 129.33, 131.11, 131.94, 132.38, 134.95 (2C), 138.32, 139.21, 139.78, 141.68, 141.77, 151.74, 151.86 (d, J = 46.8 Hz, 1C), 153.07, 163.74; HRMS (ESI^+) for $C_{27}H_{20}Cl_2FN_5O$, $[M+H]^+$ calcd: 520.1102, found: 520.1138.

***N*-[3-[[5-Chloro-2-[(*E*)-4-(3,5-dimethoxystyryl)phenylamino]-4-pyrimidinyl]amino]phenyl]-2-acrylamide (10c)**

Yield 61.3%; gray white solid; ^1H NMR (DMSO-d_6): δ 3.78 (s, 6H), 5.72-5.75 (m, 1H), 6.25-6.53 (m, 3H), 6.72-6.73 (d, J = 4 Hz, 2H), 6.94-6.98 (d, J = 16 Hz, 1H), 7.11-7.15 (d, J = 16 Hz, 1H), 7.28-7.38 (m, 4H), 7.59-7.64 (m, 3H), 7.93 (s, 1H), 8.20 (s, 1H), 9.19 (s, 1H), 9.68 (s, 1H), 10.33 (s, 1H); ^{13}C NMR (DMSO-d_6): δ 55.70 (2C), 100.03, 104.58 (2C), 116.06, 116.38, 119.48 (2C), 119.97, 126.56, 127.19 (2C), 127.39, 129.17, 129.23, 130.64, 132.43, 139.03, 139.67, 139.93, 140.18, 153.72, 153.74, 156.94, 157.03, 161.15 (2C), 163.71; HRMS (ESI^+) for $C_{29}H_{26}ClN_5O_3$, $[M+H]^+$ calcd: 528.1797, found: 528.1870.

***N*-[3-[[5-Chloro-2-[(*E*)-4-(3,5-dimethylstyryl)phenylamino]-4-pyrimidinyl]amino]phenyl]-2-acrylamide (10d)**

Yield 68.5%; light gray solid; ^1H NMR (DMSO-d_6): δ 2.28 (s, 6H), 5.73-5.76 (m, 1H), 6.25-6.30 (m, 1H), 6.50-6.57 (m, 1H), 6.89 (s, 1H), 6.96-7.07 (m, 2H), 7.17 (s, 2H), 7.24-7.26 (d, J = 8 Hz, 1H), 7.35-7.41 (m, 3H), 7.53-7.65 (m, 3H), 7.98 (s, 1H), 8.30 (s, 1H), 9.73 (s, 1H), 10.18 (s, 1H), 10.46 (s, 1H); ^{13}C NMR (DMSO-d_6): δ 21.45 (2C), 104.74, 114.29, 116.47, 117.08, 120.34, 124.59 (2C), 127.09 (2C), 127.30, 127.48, 128.08, 129.29, 129.45, 132.05, 132.40, 137.58, 138.08 (2C), 138.33, 138.60, 138.63, 139.81, 157.58, 159.15, 163.78 (2C); HRMS (ESI^+)for $C_{29}H_{26}ClN_5O$, $[M+H]^+$ calcd: 496.1899, found: 496.1962.

***N*-[3-[[5- Fluoro-2-[(*E*)-4-(3,5-dimethylstyryl)phenylamino]-4-pyrimidinyl]amino]phenyl]-2-acrylamide (10e)**

Yield 47.0%; light yellow solid; ^1H NMR (DMSO-d_6): δ 2.28 (s, 6H), 5.73-5.76 (m, 1H), 6.25-6.30 (m, 1H), 6.45-6.52 (m, 1H), 6.87-7.15 (m, 5H), 7.31-7.39 (m, 3H), 7.49-7.51 (d, J = 8 Hz, 2H), 7.69-7.71 (d, J = 8 Hz, 2H), 7.96 (s, 1H), 8.13-8.14 (d, J = 4 Hz, 1H), 9.35 (s, 1H), 9.49 (s, 1H), 10.20 (s, 1H); ^{13}C NMR (DMSO-d_6): δ 20.95 (2C), 113.69, 115.01, 117.57, 118.36 (2C), 123.95 (2C), 125.69, 126.61 (2C), 126.89, 127.98, 128.73, 129.69, 131.96, 137.31, 137.55 (2C), 138.98, 139.12, 139.37, 140.48, 140.84 (d, J = 78.8

Hz, 1C), 141.82, 149.84 (d, J = 43.6 Hz, 1C), 155.27 (d, J = 11.6 Hz, 1C), 163.15; HRMS (ESI^+) for $C_{29}H_{26}FN_5O$, $[M+H]^+$ calcd: 480.2194, found: 480.2241.

***N*-[3-[[5-Chloro-2-[(*E*)-4-(2,4-dimethylstyryl)phenylamino]-4-pyrimidinyl]amino]phenyl]-2-acrylamide (10f)**

Yield 59.7%; gray white solid; ^1H NMR (DMSO-d_6): δ 2.26 (s, 3H), 2.36 (s, 3H), 5.70-5.73 (m, 1H), 6.22-6.27 (m, 1H), 6.42-6.49 (m, 1H), 6.89-6.93 (d, J = 16 Hz, 1H), 7.00 (s, 2H), 7.13-7.17 (d, J = 16 Hz, 1H), 7.32-7.37 (m, 4H), 7.48-7.56 (m, 2H), 7.62-7.64 (d, J = 8 Hz, 2H), 7.89 (s, 1H), 8.17 (s, 1H), 9.01 (s, 1H), 9.46 (s, 1H), 10.21 (s, 1H); ^{13}C NMR (DMSO-d_6): δ 20.00, 21.23, 104.44, 116.03, 116.17, 119.24 (2C), 119.86, 123.72, 125.17, 127.05 (2C), 127.35, 127.39, 128.99, 129.16, 130.83, 131.52, 132.37, 133.79, 135.48, 136.73, 139.28, 139.57, 140.38, 155.31, 156.73, 157.96, 163.67; HRMS (ESI^+) for $C_{29}H_{26}ClN_5O$, $[M+H]^+$ calcd: 496.1899, found: 496.1954.

***N*-[3-[[5-Fluoro-2-[(*E*)-4-(2,4-dimethylstyryl)phenylamino]-4-pyrimidinyl]amino]phenyl]-2-acrylamide (10g)**

Yield 31.2%; pale yellow solid; ^1H NMR (DMSO-d_6): δ 2.26 (s, 3H), 2.36 (s, 3H), 5.70-5.77 (m, 1H), 6.23-6.29 (m, 1H), 6.93-7.01 (m, 3H), 7.15-7.19 (d, J = 16 Hz, 1H), 7.27-7.34 (m, 1H), 7.40-7.45 (m, 4H), 7.50-7.52 (d, J = 8 Hz, 1H), 7.58-7.60 (d, J = 8 Hz, 1H), 7.76-7.78 (d, J = 8 Hz, 2H), 8.13-8.14 (d, J = 4 Hz, 1H), 8.25-8.32 (m, 1H), 9.46 (s, 1H), 9.54 (s, 1H), 10.52 (s, 1H); ^{13}C NMR (DMSO-d_6): δ 19.53, 20.73, 113.13, 115.65, 117.25, 118.44, 123.01, 124.67, 126.56, 126.64 (2C), 128.66 (2C), 128.90, 130.00, 131.03, 131.93, 132.16, 133.40, 134.96, 136.17, 137.97, 139.17, 139.38, 141.66 (d, J = 81.6 Hz, 1C), 141.86, 149.75 (d, J = 43.6 Hz, 1C), 155.23 (d, J = 11.6 Hz, 1C), 163.23; HRMS (ESI^+) for $C_{29}H_{26}FN_5O$, $[M+H]^+$ calcd: 480.2194, found: 480.2229.

***N*-[3-[[5-Chloro-2-[(*E*)-4-(3,5-dichlorostyryl)phenylamino]-4-pyrimidinyl]amino]phenyl]-2-acrylamide (10h)**

Yield 60.4%; gray white solid; ^1H NMR (DMSO-d_6): δ 5.72-5.75 (m, 1H), 6.23-6.28 (m, 1H), 6.43-6.50 (m, 1H), 6.99-7.03 (d, J = 16 Hz, 1H), 7.30-7.44 (m, 6H), 7.57-7.62 (m, 5H), 7.88 (s, 1H), 8.23 (s, 1H), 9.39 (s, 1H), 9.79 (s, 1H), 10.27 (s, 1H); ^{13}C NMR (DMSO-d_6): δ 104.80, 116.33, 116.71, 119.80 (2C), 120.36, 123.78, 125.04 (2C), 126.60, 127.46, 127.63 (2C), 129.22, 130.41, 132.03, 132.28, 134.93 (2C), 138.79, 139.70, 140.34, 141.83, 156.18, 157.22, 159.19, 163.73; HRMS (ESI^+) for $C_{27}H_{20}Cl_3N_5O$, $[M+H]^+$ calcd: 536.0806, found: 536.0841.

4.3. Kinase enzymatic assays

The ADP-Glo^{TM} system ($EGFR^{WT}$, Catalog. V3831, $EGFR^{T790M/L858R}$ Catalog. V5324), purchased from Promega Corporation (USA) were used to perform the enzymatic assays. The experiments were performed according to the instructions of the manufacturer. The more detailed and complete protocols, and the active kinase data were available at: http://www.promega.com/tbs/tm313/tm313/tm313.html and http://www.promega.com/KES Protocol (or http://www.promega.com/tbs/signaling.htm), respectively. For

all of the tested compunds, concentrations consisting of suitable levels from 0.1 to 1000 nM were used. The test was performed in a 384-well plate, and includes the major steps below: (1) perform a 5 μL kinase reaction using 1×kinase buffer (e.g., 1×reactionbuffer A), (2) incubate at room temperature for 60 minutes, (3) add 5 μL of ADP-Glo™ reagent to stop the kinase reaction and deplete theunconsumed ATP, leaving only ADP and a very low background of ATP, (4) incubate at room temperature for 40 minutes, (5) add 10 μL of kinase detection, (6) reagent to convert ADP to ATP andintroduce luciferase and luciferin to detect ATP, (7) incubate at room temperature for 30 minutes, (8) plate was measured on TriStar® LB942 Multimode Microplate Reader (BERTHOLD) to detect the luminescence (Integration time 0.5-1 second). Curve fitting and data presentations were performed using GraphPad Prism version 5.0.

4.4. Cellular activity assay

H1975, H431, HCC827, and A549 human NSCLC cells were obtained from the American Type Culture Collection. HBE normal cells were kind gifts from Fuheng Biology Company (Shanghai, China). H1975, HCC827 and A549 cells were grown in RPMI-1640 (Gibco®, USA) supplemented with 10% FBS (Gibco®, USA), 1% penicillin-streptomycin (Beyotime Company, China). A431 and HBE cells were grown in DMEM (Gibco®, USA) supplemented with 10% FBS (Gibco®, USA), 1% penicillin-streptomycin (Beyotime Company, China). All cells were maintained and propagated as monolayer cultures at 37 °C in humidified 5% CO_2 incubator.

Cell viability was then assessed with MTT reagent (Thiazolyl blue tetrazolium bromide; Sigma, Oakville, ON). Cells were seeded in 96-well plates at a density of 3,000 to 5,000 cells/well and were maintained at 37 °C in a 5% CO_2 incubator in DMEM or RPMI1640 containing 10% fetalbovine serum (FBS, Gibico). Cells were esposed to treatment for 72 h, and the number of cells used per experiment for each cell line was adjusted to obtain an absorbance of 0.5 to 1.2 at 570 nm. Compounds were tested at appropriate concentrations (0.01 to 40 μM), with each concentration duplicated five times. The data were calculated using GraphPad Prim version 5.0. Dose-response curves were fitted using a nonlinear regression model with a sigmoidal dose-response.

4.7. Molecular docking study

AutoDock 4.2.6 software was used to carry out the docking studies. Detailed tutorials that guide users through basic AutoDock usage, docking with flexible rings, and virtual screening with AutoDock may be found at: http://autodock.scripps.edu/faqs-help/tutorial. Generally, the crystal structure (PDB: 3IKA) of the kinase domain of $EGFR^{T790M}$ bound to inhibitor **4** was used in the docking studies. The enzyme preparation and the hydrogen atoms adding was performed in the prepared process. The whole EGFR enzyme was defined as a receptor and the site sphere was selected on the basis of the binding location of WZ4002. By moving WZ4002 and the irrelevant water, molecule **10e** was placed**.** The binding interaction energy was calculated to include Van der Waals, electrostatic, and torsional energy terms defined in the tripos force

field. The structure optimization was performed using a genetic algorithm, and only the best-scoring ligand protein complexes were kept for analyses.

Acknowledgements

We are grateful to the National Natural Science Foundation of China (No. 81402788), and the Cultivation Project of Youth Techstars, Dalian, 2016RQ043) for the financial support of this research.

Reference

1. Jemal, A.; Siege, R.; Ward, E.; Hao, Y.; Xu, J.; Thun, M.J. *CA Cancer J Clin.* **2009**, *59*, 225.
2. Siegel, R.; Naishadham, D.; Jema, A. *CA Cancer J Clin.* **2013**, *63*, 11.
3. Yang, P.; Allen, M. S.; Aubry, M. C.; Wampflerd, J. A.; Marks, R. S.; Edell, E. S.; Thibodeau, S.; Adjei, A. A.; Jett, J.; Deschamps, C. *Chest* **2005**, *128*, 452.
4. Raez, L. E.; Kobina, S.; Santos, E. S. *Clin. Lung Cancer* **2010**, *11*, 18.
5. Ramalingam, S. S.; Khuri, F. R. *Oncologist* **2009**, *14*, 412.
6. Ramalingam, S.; Belani, C. P. *Expert Opin. Pharmaco.* **2002**, *3*, 1693.
7. Nicola, N.; Antonella, D. L.; Caterina, B.; Luigi, L.; Mario, M.; Maiello, M. R.; Adele, C.; Gianfranco, D. F.; Francesco, C.; Salomon, D. S. *Gene* **2006**, *366*, 2.
8. Carpenter, G.; Cohen, S. *J. Biol. Chem.* **1990**, *265*, 7709.
9. Gazdar, A. F. *Oncogene* **2009**, *28*, S24.
10. Shigematsu, H.; Li, L.; Takahashi, T.; Nomura, M.; Suzuki, M.; Wistuba, I. I.; Fong, K. M.; Huei, L.; Toyooka, S.; Shimizu, N.; Fujisawa, T.; Feng, Z.; Roth, J. A.; Herz, J.; Minna, J. D.; Gazdar, A. F. *J. Nat. Cancer Inst.* **2005**, *97*, 339.
11. Vansteenkiste, J. *Expert Rev. Anticancer Ther.* **2004**, *4*, 5.
12. Tiseo, M.; Loprevite, M.; Ardizzoni, A. *Curr. Med. Chem: Anti-Cancer Agents* **2004**, *4*, 139.
13. Bonomi, P. *Expert Opin. Investig. Drugs* **2003**, *12*, 1395.
14. Lee, J.; Hahn, S.; Kim, D.; Suh, K.; Keam, B.; Kim, T.; Lee, S.; Heo, D. *JAMA.* **2014**, *311*, 1430.
15. Ercan, D.; Choi, H.; Yun, C.; Capelletti, M.; Xie, T.; Eck, M. J.; Gray, N. S.; Janne, P. A. *Clin. Cancer Res.* **2015**, *21*, 3913.
16. Kobayashi, S.; Boggon, T.; Dayaram, T.; Janne, P. A.; Kocher, O.; Meyerson, M.; Johnson, B. E.; Eck, M. J.; Tenen, D. G.; Halmos, B. *N. Engl. J. Med.* **2005**, *352*, 786.
17. Kwak, E. L.; Sordella, R.; Bell, D. W.; Godin-Heymann, N.; Okimoto, R. A.; Brannigan, B. W.; Harris, P. L.; Driscoll, D. R.; Fidias, P.; Lynch, T. J.; Rabindran, S. K.; McGinnis, J. P.; Wissner, A.; Sharma, S. V.; Isselbacher, K. J.; Settleman, J.; Haber, D. A. *Proc. Natl. Acad. Sci. U.S.A.* **2005**, *102*, 7665.
18. Silva, A. P.; Coelho, P. V.; Anazetti, M. *Hum. Vaccin. Immunother.* **2016**, *101*, 12.
19. Zhou, W.; Ercan, D.; Chen, L.; Yun, C.; Li, D.; Capelletti, M.; Cortot, A. B.; Chirieac, L.; Iacob, R. E.; Padera, R.; Engen, J. R.; Wong, K.; Eck, M. J. ; Gray, N. S.; Janne, P. A. *Nature* **2009**, *462*, 1070.

20. Walter, A. O.; Tjin Tham Sjin, R.; Haringsma, H. J.; Ohashi, K.; Sun, J.; Lee, K.; Dubrovskiy, A.; Labenski, M.; Zhu, Z.; Wag, Z.; Sheets, M.; St Martin, T.; Karp, R.; Van Kalken, D.; Chaturvedi, P.; Niu, D.; Nacht, M.; Petter, R. C.; Westlin, W.; Lin, K.; Jaw-Tsai, S.; Raponi, M.; van Dyke, T.; Etter, J.; Weaver, Z.; Pao, W.; Singh, J.; Simmons, A. D.; Harding, T. C.; Allen, A. *Cancer Discov*. **2013**, *3*, 1046.

21. Cross, D. A.; Ashton, S. E.; Ghiorghiu, S.; Eberlein, C.; Nebhan, C. A.; Spitzler, P. J.; Orme, J. P.; Finlay, M. R.; Ward, R. A.; Mellor, M. J.; Hughes, G.; Rahi, A.; Jacobs, V. N.; Red Brewer, M.; Ichihara, E.; Sun, J.; Jin, H.; Ballard, P.; Al-Kadhimi, K.; Rowlinson, R.; Klinowska, T.; Richmond, G. H. P.; Cantarini, M.; Kim, D. W.; Ranson, M. R.; Pao, W. *Cancer Discov.* **2014**, *4*, 1404.

22. Finlay, M. R-V.; Anderton, M.; Ashton, S.; Ballard, P.; Bethel, P. A.; Box, M. R.; Bradbury, R. H.; Brown, S. J.; Butterworth, S.; Campbell, A.; Chorley, C.; Colclough, N.; Cross, D-A. E.; Currie, G. S.; Grist, M.; Hassall, L.; Hill, G. B.; James, D.; James, M.; Kemmitt, P.; Klinowska, T.; Lamont, G.; Lamont, S. G.; Martin, N.; McFarland, H. L.; Mellor, M. J.; Orme, J-P.; Perkins, D.; Perkins, P.; Richmond, G.; Smith, P.; Ward, R-A.; Waring, M-J.; Whittaker, D.; Wells, S.; Wrigley, G. L. *J. Med. Chem.* **2014**, *57*, 8249.

23. Park, E. J.; Pezzuto, J. M. *Biochim. Biophys. Acta* **2015**, *1852*, 1071.

24. Zakharov, S.; Smani, T.; Dobrydneva, Y.; Bolotina, V. M. *Biophys. J*. **2004**, *86*, 430A.

25. Xie, B.; Xu, Z.; Hu, L.; Chen, G.; Wei, R.; Yang, G.; Li, B.; Chang, G.; Sun, X.; Wu, H.; Zhang, Y.; Dai, B.; Tao, Y.; Shi, J.; Zhu, W. *Int. J. Mol. Sci.* **2016**, *17*, 11.

26. Song, Z.; Jin, Y.; Ge, Y.; Wang, C.; Zhang, J.; Tang, Z.; Peng, J.; Liu, K.; Li, Y.; Ma, X. *Bioorg. Med. Chem*. **2016**, *24*, 5505.

27. Zhao, D.; Huang, S.; Qu, M.; Wang, C.; Liu, Z.; Li, Z.; Peng, J.; Liu, K.; Li, Y.; Ma, X.; Shu, X. *Eur. J. Med. Chem*. **2017**, *126*, 444.

28. Ge, Y.; Jin, Y.; Wang, C.; Zhang, J.; Tang, Z.; Peng, J.; Liu, K.; Li, Y.; Zhou, Y.; Ma, X. *ACS Med. Chem. Lett*. **2016**, *7*, 1050.

29. Zegzouti, H.; Zdanovskaia, M.; Hsiao, K.; Goueli, S. A. *Assay Drug Dev. Technol.* **2009**, *7*, 560.

30. Wildman, S. A.; Zheng, X.; Sept, D.; Auletta, J. T.; Rosenberry, T. L.; Marshall, G. R. *Chem. Biol. Drug Des*. **2011**, *78*, 495.

31. Morris, G. M.; Huey, R.; Lindstrom, W.; Sanner, M. F.; Belew, R. K.; Goodsell, D. S.; Olson, A. J. *J. Comput. Chem.* **2009**, *16*, 2785.

32. Liu, H.; Dong, A.; Gao, C.; Tan, C.; Liu, H.; Zu, X.; Jiang, Y. *Bioorg. Med. Chem.* **2008**, *16*, 10013.

33. Lu, C.; Guo, Y.; Yan, J.; Luo, Z.; Luo, H. B.; Yan, M.; Huang, L.; Li, X. *J. Med. Chem.* **2013**, *56*, 5843.